MACHINE STABILITY AND ORBIT CORRECTION IN ELETTRA

R. Nagaoka*
Sincrotrone Trieste, Padriciano 99, 34012 Trieste, Italy

Abstract

The paper describes recent progress made in ELETTRA on the orbit correction, both locally and globally, to improve the orbit stability as well as the correction efficiency.

1. INTRODUCTION

After the commissioning stage, the orbit correction in ELETTRA has been progressing in two directions. One is to guarantee the orbit stability at a source point of each insertion device, where the major orbit variation is found to be a slow drift due to machine stability. High level software is used to perform a slow feed back by means of local bumps. To achieve a correction level of microns with no disturbance elsewhere, correctors are firstly calibrated to create bumps empirically so that they are rigorously closed. Furthermore, a 4-corrector bump is extended to a 5-corrector bump in the horizontal plane to overcome the variation of path length which affects the orbit globally. The second direction is to improve the efficiency and the quality of global corrections. Application of the SVD method and a simultaneous correction of orbit and spurious dispersion are developed.

2. SLOW LOCAL ORBIT FEED BACK

At every user operation, the orbit displacement and its slope at the centre of an insertion device (ID), as interpolated from the two adjacent BPMs [1], are compensated to zeros in each plane using a 4-corrector bump, prior to delivering light or whenever an orbit drift is encountered. As the ELETTRA BPMs have the relative reading accuracy of few microns [2], the correction is made down to the level of microns and microradians. To facilitate this procedure, previous manual correction using Bump [1] had been taken over by a high level software program SlowFB [3], which performs an automatic correction at every specified time interval in all insertion device sections specified by clicking on the toggle buttons on the control panel. Correction in a section is activated whenever an orbit is detected to be above a predefined threshold. Several upper limits are set inside the program to avoid risky actions caused by possible erroneous readings of BPMs and correctors.

What encountered upon applying the slow feed back was that, despite its higher efficiency, it requires a number of iterations to converge which is not only due to corrections within one section but rather to additional distortion generated by bump leakage in other sections. In fact, there arose complaints from the users that they are disturbed during the correction procedure. This aspect was clearly worsening as the number of activated sections was increased, and at the limit of activating all eleven sections the correction was observed to even diverge.

To overcome this difficulty, a scheme had been developed to replace the corrector strengths calculated using the model optics by those derived through an empirically obtained relation which ensures the bump closure. The four corrector angles $\Delta\theta_j$ (j = 1,...,4) are related linearly to the desired changes Δu and $\Delta u'$ at the bump location in terms of eight coefficients a_{1j} and a_{2j}:

$$\Delta\theta_j \equiv a_{1j}\cdot\Delta u + a_{2j}\cdot\Delta u', \qquad (1)$$

which can be expressed analytically. The problem is therefore to calibrate the coefficients empirically, which is achieved by 'closing' the bumps for two cases; i) $\Delta u \neq 0$ and $\Delta u' = 0$. ii) $\Delta u = 0$ and $\Delta u' \neq 0$. The developed procedure iterates the matrix inversion, which we shall describe for the case i): Let *i* represent three monitors with *i* = 1 and 3 being outside the bump on each side, and *i* = 2 at the bump location, and let $\Delta u_i(k)$ be the difference with respect to the initial orbit observed by the *i*th monitor at *k*th iteration. The corrector increment $\Delta\theta_j(k)$ at *k*th iteration should satisfy

$$\begin{aligned}
\sum_j A_{ij}\cdot\Delta\theta_j(k) &= -\Delta u_i(k), \quad (i = 1 \text{ and } 3)\\
\sum_j A_{2j}\cdot\Delta\theta_j(k) &= \Delta u - \Delta u_2(k), \qquad (2)\\
\sum_j B_{2j}\cdot\Delta\theta_j(k) &= -\Delta u'_2(k),
\end{aligned}$$

where A_{ij} and B_{ij} are the familiar closed orbit formulae,

$$A_{ij} = \frac{\sqrt{\beta_i\beta_j}}{2\sin\pi Q}\cdot\cos\Theta_{ij}, \quad (\Theta_{ij} = \pi Q - |\psi_i - \psi_j|)$$

$$B_{ij} = \pm\frac{\sqrt{\beta_i/\beta_j}}{2\sin\pi Q}\,(\sin\Theta_{ij} \mp \alpha_i\cdot\cos\Theta_{ij}) \qquad (3)$$

in which the upper sign corresponds to $\psi_i > \psi_j$ and the lower sign, to $\psi_i < \psi_j$. Other symbols have the usual meanings. The iteration is continued until a required convergence level is achieved. The final corrector strength $\Delta\theta_j$ is obtained by adding up $\Delta\theta_j(k)$. The procedure for ii) is in complete analogy to i). In the real application, the calibration converges rapidly normally within several iterations to the level of microns, however it depends much on the beam stability which affects the BPM readings. To demonstrate the effectiveness of the empirical bumps, the result of a vertical correction activated in all eleven sections is compared in Fig. 1 with the conventional method using the model optics.

---

*Present address: ESRF, BP220, F-38043 Grenoble Cedex, France, which supports the presentation of this work.

The same, however, was not true in the horizontal plane, which was due to a global orbit distortion that occurs even though the calibration itself converges equally

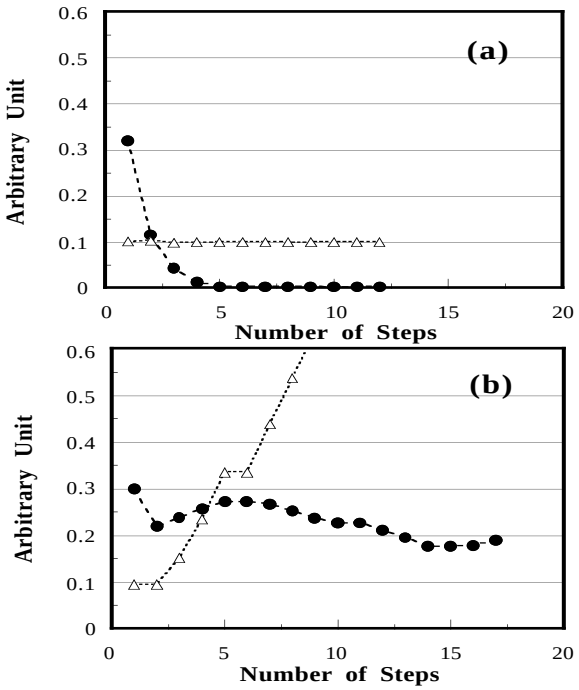

Fig. 1. Norm as defined by $y^2 + (\beta \cdot y')^2$ versus correction steps in (a) empirical and (b) conventional correction. Circles are the sum over all 11 correcting ID sections, while triangles are at the non-correcting injection section, respectively.

well as the other plane. This strange behaviour was understood to be due to a path length distortion caused by one of the correctors which is the only one out of four sitting in the dispersive section, while we know that the path length is shifted proportionally to the product of a corrector kick angle and the dispersion at the corrector position [1]. The encountered difficulty was removed by adding an adjacent corrector which also sits in the dispersive section to make a 5-corrector bump thereby imposing a constraint on top of Eqs. 2 to keep the path length unchanged: $\sum_{1,5} D_j \cdot \Delta\theta_j(k) = 0$ where D_j denotes the horizontal dispersion. This extension has been confirmed to work successfully in both the calibration procedure and the correction. However, there appears to be a reduction in the valid correction range as well as degradation in the convergence rate, the reason of which is yet to be analysed

Regarding the effect of path length, a simulation code had been extended to take it into account so that a sudden shift in the beam energy due to a change in the corrector strength or in the rf frequency can be simulated. The existing six-dimensional tracking routine in an extended version of RACETRACK [4] is utilised to compute the path length deviation $d\sigma$ of a given closed orbit x_{co} with respect to the nominal circumference L, which is generally composed of two contributions,

$$d\sigma = -\oint \frac{x_{co}}{\rho}\, ds - \delta \cdot \alpha \cdot L \qquad (4)$$

where ρ is the bending radius, $\delta = \Delta p/p_0$ is a momentum offset, and α denotes the momentum compaction. A positive $d\sigma$ signifies a shortening. If $d\sigma$ is not equal to the shift defined by the rf frequency $\Delta f_{rf}/f_{rf} \cdot L$, the electrons will shift their energy by

$$\delta_{new} = \delta_{old} + \frac{1}{\alpha}\left(\frac{d\sigma}{L} - \frac{\Delta f_{rf}}{f_{rf}}\right) \qquad (5)$$

to satisfy the equality. The simulation code will iterate the computation of Eqs. 5 and 6 until a closed orbit is found at which convergence is achieved.

3. GLOBAL ORBIT CORRECTIONS

Two routines, the SVD (Single Value Decomposition) method and a dispersion correction have been additionally implemented into the program Orbit [5]. The correction of spurious dispersion had been found to be particularly important for ELETTRA due to high sensitivity against orbit errors. The correction is made by using the steerers with the sensitivity matrix prepared for the dispersion, the details of which are described in Ref. 6.

The feature which makes the SVD method particularly attractive is, as known, to be able to discard small eigenvalues which generally cause large corrector kicks only to make minor improvements on the orbit [7]. One can thus make a stepwise approach as in the best corrector method, by proceeding with larger eigenvalues in the matrix inversion. The number of eigenvalues therefore becomes a key parameter to be adjusted. The superiority of the method has been proven in ELETTRA as well, in its efficiency, i.e. the fast convergence, and in keeping the corrector strength markedly low compared to other methods under the same level of the orbit rms. In the 82 $\times$ 96 corrector-BPM system of ELETTRA, the correction usually saturates with the number of eigenvalues around 20. The resultant corrector strengths are typically ~0.2 mrad rms horizontally and ~0.1 mrad rms vertically.

With the great effectiveness of the method shown in the orbit correction, it had also been applied to the dispersion correction where again it was found to be equally effective leading to the most recent development which extends the method to perform a simultaneous correction of both orbit and dispersion. The scheme consists simply of doubling the monitor (BPM) dimension;

$$\begin{bmatrix} \kappa\mathbf{A} \\ \mathbf{D} \end{bmatrix} \cdot \mathbf{x} = \begin{bmatrix} \kappa\mathbf{y} \\ \mathbf{d} \end{bmatrix} \qquad (6)$$

Here, **A** and **D** represent sensitivity matrices for the orbit and the dispersion, respectively, **x** is an array containing *N* corrector strengths, and **y** and **d** denote vectors composed of orbit and dispersion values at *M* BPMs, respectively. An adjustable parameter κ is introduced to be able to vary the relative amplitude of eigenvalues of one matrix to those of the other, which therefore determines the weighting between the correction of the two quantities. The adjustment is actually handled by defining

$\kappa_0 \cdot \alpha_{max} \equiv \delta_{max}$ and $\kappa \equiv \eta \cdot \kappa_0$, where α_{max} and δ_{max} represent the maximum eigenvalues of **A** and **D**, respectively, and η is a variable in the range $\eta \geq 0$. The case in which η is unity treats orbit and dispersion on equal weighting, while $\eta \rightarrow 0$ limit corresponds to correcting only the dispersion, and $\eta >> 1$ limit, on the contrary to the orbit correction. With a scroll bar on the control panel one can vary continuously η from zero to the maximum set to ten, passing through one at the centre. The distribution of eigenvalues are compared in Fig. 2 for the above three distinctive cases in ELETTRA, in the vertical plane. The values are normalised to the maximum eigenvalue in each case. It is seen that the eigenvalues of **A** decay faster than those of **D**, and that

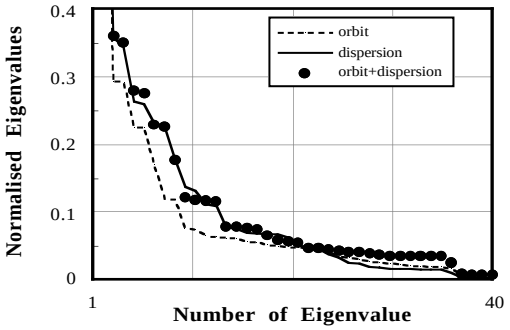

Fig. 2. Distribution of eigenvalues for three different cases: 1) $\eta >> 1$ (dashed line). 2) $\eta = 0$ (solid line). 3) $\eta = 1$ (dark circles).

those of the combined matrix have a slower decay as expected. In the horizontal correction, one can straightforwardly impose a constraint to keep the path length distortion due to correctors to zero in the similar way as above, by adding a row $\xi \cdot \mathbf{D_h} \cdot \mathbf{x} = 0$ to Eq. 7, where $\mathbf{D_h}$ is an array containing the dispersion values at correctors, and ξ is a variable like κ, adjusted to make an appropriate weighting with respect to the rest of the equations. This simple introduction of the important constraint should clearly be another advantage of the matrix inversion approach.

To study the effectiveness of the extended scheme, application has been made to ELETTRA for the three distinctive cases; $\eta = 0$, 1 and 10 for comparison, starting from the same condition. Although in the shown example in the vertical plane (Figs. 3), there are no marked differences in the final values, there is a trend that the simultaneous correction ($\eta = 1$) brings both orbit and dispersion rms's to lower values, as well as that other cases leave the rms of the uncorrecting part larger than the correcting ones. In terms of number of eigenvalues, the simultaneous correction saturates round 40 which is twice as large as those in the usual orbit or dispersion corrections.

In the horizontal plane, we encounter a large mismatch between the orbit and the dispersion which becomes clearer as the correction proceeds, and appears to be beyond the context of the correction. It may be due to horizontal mispositioning of the machine components caused possibly by the heat load. The path length constraint is found to be fulfilled by taking values such as ~100 for ξ for ELETTRA.

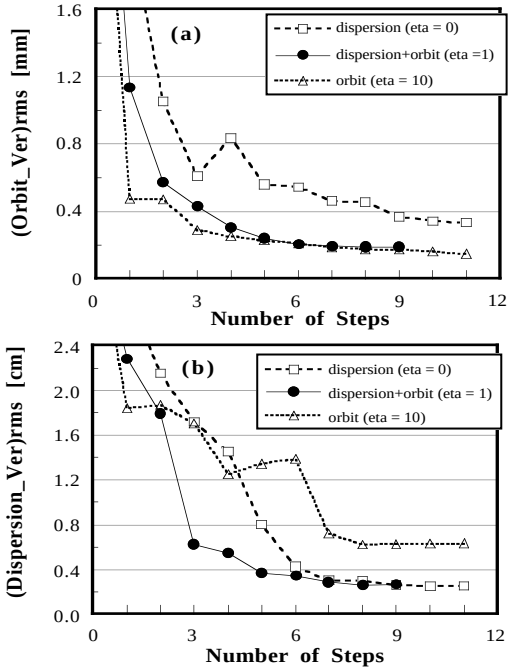

Fig. 3. The rms of (a) orbit and (b) dispersion versus number of correction steps for three different cases: 1) $\eta = 0$ (squares). 2) $\eta = 1$ (circles). 3) $\eta = 10$ (triangles).

The SVD method has also been implemented and used successfully in an automatic orbit correction routine [3] which has recently been developed to help stabilise the orbit globally during user operations.

4. ACKNOWLEDGEMENT

The author thanks C.J. Bocchetta, A. Fabris, F. Iazzourene, E. Karantzoulis, M. Svandrlik, L. Tosi, R.P. Walker, A. Wrulich and all other ELETTRA shift crew for their contribution in the machine operation and measurements.

5. REFERENCES

[1] R. Nagaoka et al., "Orbit Correction in ELETTRA", Proc. 4th EPAC, London, June 1994, p.1009.
[2] R. De Monte et al., "Elettra BPM System", Proc. 4th EPAC, London, June 1994, p.1530.
[3] R. Nagaoka, to appear as an internal note.
[4] R.Nagaoka, "Effect of Coupled Synchro-Betatron Oscillation in the ELETTRA Storage Ring", ST/M-91/20, Sincrotrone Trieste (1991); A. Wrulich, "RACETRACK", DESY report 84-026 (1984).
[5] R. Nagaoka, "Orbit V1.0 User's Manual", ST/M-TN-93/12, Sincrotrone Trieste (1993).
[6] R. Nagaoka, "Coupling and Dispersion Correction in ELETTRA", this conference.
[7] Y. Chung et al., "Global DC Closed Orbit Correction Experiment on the NSLS X-ray Ring", ANL LS-213 (1992) .